Molecular Crystals and Liquid Crystals
Publication details, including instructions for authors and subscription information:
http://www.tandfonline.com/loi/gmcl16

Elastic Deformations and Electrohydrodynamic Instabilities in Large Pitch Cholesteric Liquid Crystals under an Electric Field

M. L. Sartirana [a], B. Valenti [a] & R. Bartolino [a]
[a] Istituto di Chimica Industrigle, Università di Genova, Genova (Italia), Dipartimento di Fisica, Università delta Calabria, Cosenza, (Italia)
Version of record first published: 17 Oct 2011.

To cite this article: M. L. Sartirana , B. Valenti & R. Bartolino (1983): Elastic Deformations and Electrohydrodynamic Instabilities in Large Pitch Cholesteric Liquid Crystals under an Electric Field, Molecular Crystals and Liquid Crystals, 98:1, 321-347

To link to this article: http://dx.doi.org/10.1080/00268948308073485

Mol. Cryst. Liq. Cryst., 1983, Vol. 98, pp. 321–347
0026-8941/83/9804–0321/$18.50/0

Printed in the United States of America

Elastic Deformations and Electrohydrodynamic Instabilities in Large Pitch Cholesteric Liquid Crystals under an Electric Field†

M. L. SARTIRANA, B. VALENTI and R. BARTOLINO‡

Istituto di Chimica Industriale, Università di Genova, Genova (Italia),
‡Dipartimento di Fisica, Università della Calabria, Cosenza (Italia)

(Received February 18, 1983)

We report experimental observations on large pitch cholesteric liquid crystals in the planar geometry submitted to DC or low frequency AC fields applied along the helical axis. An electric field can cause orientation of the molecules in the field direction (tilting of the helical axis leading to a fingerprint texture and unwinding of the cholesteric spiral) or disruption of the orientation due to the hydrodynamic effect of current carriers (periodic two-dimensional deformations). The behavior of the samples depends upon the sign and the absolute value of the dielectric anisotropy ε_a. We have investigated a wide range of systems by using nematic matrices with ε_a between -4 and $+33$ doped with small amounts of cholesteryl chloride ($\varepsilon_a > 0$) and cholesteryl benzoate ($\varepsilon_a < 0$).

Instabilities are observed in negative ε_a mixtures; depending upon the frequency, two regimes can be found, as in nematics. The behavior above threshold depends largely on the magnitude of the negative anisotropy. In the case of a small positive ε_a, domain instabilities and elastic deformations occur. The nature and the amount of the cholesteric dopant affect the threshold for the square grid deformation. The response of mixtures with strong ε_a involves processes in which the orientation of the molecules by the field is the principal effect. Upon increasing the voltage, the instabilities of the nematic phase in the homeotropic geometry appear in the form of a conduction and a dielectric regime of splay. The Frank elastic constants are derived from the threshold field of the different deformations.

---

†Presented at the Ninth International Liquid Crystal Conference, Bangalore, December 6–10, 1982.

INTRODUCTION

The behavior of cholesteric liquid crystals in an electric field is generally far less well explained than that for nematics. Some basic effects have been elucidated, but although intensive investigations have been devoted to this topic in the last decade,[1] many questions remain unanswered because of the rather complex nature of the phenomena. Technological applications of cholesteric electro-optical effects have not as yet been extensively realized; this is because of the reasons just described and the difficulty in obtaining samples that are uniformly oriented (single crystals). Reports on the electric conductivity are still incomplete at present, but some results indicate that ionic transport may be the dominant conduction mechanism in the cholesteric phase of cholesteryl esters.[2] A number of investigations of the dielectric properties of cholesterics are reported in the literature,[1] but their interpretation is often difficult because of the confusing influence of the texture. It should be realized that $\varepsilon_a = \varepsilon_\parallel - \varepsilon_\perp$ is positive for cholesteryl halides and negative for cholesteryl esters[3] ($\varepsilon_\parallel$ and $\varepsilon_\perp$ are the dielectric constants measured respectively parallel and perpendicular to the molecular axis).

An analogy with the behavior of nematics may provide some useful means for interpreting the electro-optical effects of cholesterics. The main results can be summarized as follows:

- In the case of negative ε_a the cholesteric sample minimizes its energy by aligning the helical axis with the field. This effect can be observed in A. C. by doping MBBA with cholesterol esters;[4] beyond a certain frequency, the convective instabilities are eliminated and a well ordered planar texture is obtained. Instabilities have also been studied under AC fields; depending on the frequency, two regimes can be found, as in the case of negative nematics in a planar texture.[5,6]
- Cholesteric samples with positive ε_a tend to adjust the helical axis normal to the applied field. Experimentally, a cholesteric liquid crystal in the planar texture goes to the focal-conic texture because of a 90° rotation of the helical axis.[7] As the field strength approaches a critical value E_{CN}, the pitch increases logarithmically; for $E > E_{CN}$ the helix is destroyed completely and the structure becomes nematic.[8,9] In the original experiments on cholesterol derivatives, the pitch was small, the threshold voltage high, and the spatial periodicity too small for direct optical observation. The phenomena can be studied more accurately in the case of nematic/cholesteric mixtures where the pitch is large.

Another possible mechanism must be considered for the disappearance of the helical structure in an electric field: the expansion of the helix due

to a conical deformation.[10] In this case, the field acts parallel to the helical axis and the helix is extinguished by a reduction of the angle between its axis and that of the molecules (the cholesteric pseudo-layers intersect each other). However, numerous cholesterics do not undergo such a transformation; prerequisites for this process are a positive ε_a and the relation $K_{22} > K_{33}$ between the elastic constants for twisting and bending.

Recently Bartolino, *et al.*,[11] have carried out coupled capacitance and optical measurements showing that in the same sample of a small pitch cholesteric, different deformations occur at different values of a DC electric field applied parallel to the helical axis. They found a definite hierarchy for the onset of different deformations in the case of a sample thickness much larger than the cholesteric pitch.

The aim of this work is the investigation of the orientation effects and of the electric field-induced instabilities in cholesteric liquid crystals of different ε_a. To increase the size of the distortions and decrease the threshold voltages we investigated nematic/cholesteric mixtures of large pitch prepared by doping nematic liquid crystals with small amounts of cholesteryl chloride CC ($\varepsilon_a > 0$) and cholesteryl benzoate CB ($\varepsilon_a < 0$). The cases of both negative and positive dielectric anisotropy were investigated, since the experiments were carried out with negative and positive nematics. Most of the results agree satisfactorily with theoretical predictions and experimental reports, and allow a determination of some elastic constants of pure nematics. The most interesting situation appears to be the limiting one $\varepsilon_a \simeq 0$.

EXPERIMENTAL

The nematic phases studied are schematically indicated in Table I and are the same as those investigated in previous work concerning the effect of dielectric anisotropy on the behavior of nematic liquid crystals in an electric field.[12] The CC sample was obtained from FLUKA AG and the CB sample from Riedel de Haën AG.

Nematic/cholesteric mixtures of different compositions were prepared by weighing the two components in a glass tube and heating in an oven up to the clearing point.

The compositions, pitches and handedness of the mixtures are reported in Table I. The pitches were derived using the Grandjean-Cano wedge technique from the positions of the discontinuity lines,[3,13–16] observed with a polarizing microscope (Reichert-Zetopan). The accuracy is not better than 10%. The handedness of the helices was obtained by observing the displacement of the extinction rings, connected with the variation of the rotatory power with thickness, induced by rotation of the analyzer.[17]

Table I

Nematic/Cholesteric Mixtures

Nematic Phase	CC, w/w%	CB, w/w%	Pitch, μm	Constant ($P \cdot c$)	Handedness
S1014	1		13.5	0.133 ± 0.001	right
($\varepsilon_a = -4.0$)†	3.8		3.5		right
		1.5	6.5	0.049 ± 0.001	right
		3.1	3		right
MBBA	1		21.0	0.23 ± 0.02	left
($\varepsilon_a = -0.62, 22^0$)	2		12.5		left
	4		6.0*		
	8		3.0*		
		1	24.0	0.25 ± 0.02	left
		2	13.5		left
		10	2.5*		
NP1052	1		22.0	0.235 ± 0.015	left
($\varepsilon_a = +0.1, 20^0$)	2		12.5		left
	5		5.7**	—	
	10		4.3**	—	
		1	14.0	0.16 ± 0.02	left
		2	9.0		left
		6	3.0*		
		10	1.5*		
PEBAB	1		100	1	
($\varepsilon_a = +15.5, 125^0$)	10		10		
		4	10	0.4	
		10	4		
S1016		2.9	24	0.688 ± 0.08	
($\varepsilon_a = +33.0$)†		4	17		

*Values calculated from $P \cdot c$ = constant

**These values are larger than predicted by the simple equation $P \cdot c$ = constant, probably due to a saturation effect at higher concentrations of the cholesteric dopant.

†Values extrapolated from results obtained with room temperature solutions in an eutectic mixture of azoxy compounds.

CC and CB bestow a different twist upon nematic phases. When a small concentration of an optically active dopant is dissolved in a nematic, the resulting pitch can be defined[3] as

$$P = 1/C_w P_t \tag{1}$$

where C_w is the weight concentration and P_t the macroscopic twisting power of the dopant.[3,18] Pure CC is right-handed ($P_t = +2.96$), while pure cholesteryl esters are left-handed ($P_t < 0$). Applying Eq. 1 to our systems, we obtain pitch values which generally differ from the data in Table I. In addition, therefore, a significant effect of the achiral molecules of the nematic host must be considered.

Pitch vs composition can be calculated quite accurately if it is assumed that the nematic is passive. Some cholesteric mixtures show a linearly additive effect of the helical twisting power or inverse pitch of the two components on a weight basis.[19] However, many systems composed of cholesteric and nematic compounds do not obey such a linear law. These systems can be treated by including first order interaction terms. MBBA/CC mixtures are consistent with this model.[20–22] Thus it is also necessary to ascribe a "helical twisting power" to the achiral nematic.[23]

An electro-optical cell consisting of two parallel coated plates held apart by insulating mica spacers of thickness L was used to study electrical realignment. The liquid crystals were introduced by capillarity between the rubbed electrodes and the electric field was directed normal to the layers which exhibited the planar texture with oily streaks. The cells were placed between crossed polarizers (the microscope was equipped with a Mettler FP-52 electrically heated hot-stage) and submitted to DC and low frequency AC fields, as described elsewhere.[12] Care was taken to avoid geometries with $P/L \geqslant 1$.

RESULTS AND DISCUSSION

(a) Negative dielectric anisotropy.

In the case of nematic/cholesteric mixtures of negative ε_a a good planar cholesteric texture can be obtained using preliminary rubbing of the electrodes followed by dielectric alignment at high frequency and voltage. An electric field applied parallel to the helical axis causes, below a critical frequency ω_c (conduction regime), a periodic bending of the cholesteric planes. Above the threshold, the undulations build up a square grid pattern (undulation of the layers along two orthogonal directions). Beyond the cut-off frequency, in the dielectric regime, the distortions which take place at threshold are time-dependent; we observe domain instabilities in the form of a square grid of focal units having a shorter period (in a few μm range) than in the frequency region below ω_c. These effects are observed both with small and large negative dielectric anisotropy (doped MBBA and S1014). The analogy with the behavior of undoped nematics is striking.

As a small negative ε_a cholesteric, we chose doped MBBA and report just a few data to compare with those which are described in the literature;[5,6] our results agree quite well with such reports. Figure 1 refers to the room temperature frequency dependence of the threshold fields for two mixtures where the same amount of CC is dissolved in two MBBA samples differing

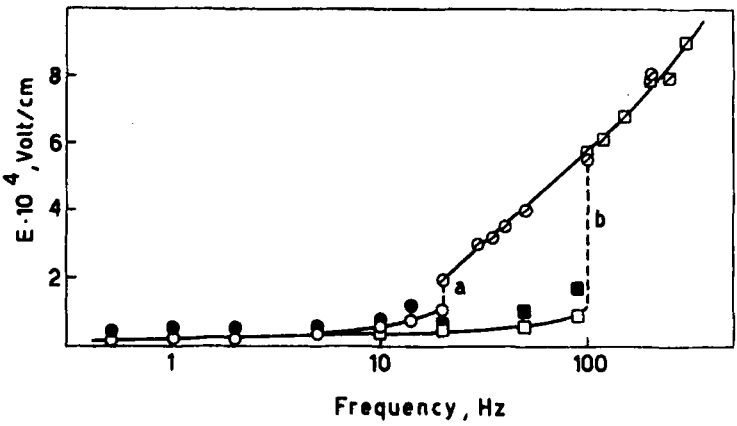

FIGURE 1 Frequency dependence of the threshold fields for MBBA/2% CC mixtures; curve a: fresh sample, curve b: sample of increased conductivity due to ageing (room temperature, $L = 20\ \mu m$). ○ □ square grid pattern, ● ■ polygonal texture, ⊘ ⧄ dielectric regime.

in ageing (curve a: fresh sample, curve b: sample of increased conductivity due to ageing). Microscopic observations at threshold on a mixture of MBBA/CC are shown in Figure 2. The low frequency mode, corresponding to the static square grid, is replaced by the tilted polygonal texture nucleated from the centers of the squares[24] as the field is raised to about double the threshold. This resulting state is metastable and relaxes slowly to the planar texture if the field is switched off. However, it is possible to accelerate the recovery of the planar texture by applying a signal of frequency in the range of the dielectric regime. At higher voltages, turbulence sets in and the system reaches the dynamic scattering mode. On turning off the field, the liquid crystal relaxes to the polygonal texture.

The theory of the square grid deformation was proposed by Helfrich[25,26] and subsequently elaborated by Hurault,[27] who discussed the threshold condition in a cholesteric planar texture of pitch P_o and thickness L under AC fields. The frequency dependence of the threshold field is quite similar to the one predicted for nematics[28,29] and is given by

$$E_H^2(\omega) = \frac{8\pi^3}{\varepsilon_\perp}\frac{\varepsilon_\perp + \varepsilon_\parallel}{\varepsilon_\perp - \varepsilon_\parallel}\frac{1 + \omega^2\tau^2}{\zeta - 1 - \omega^2\tau^2}\left(\frac{3}{2}K_{22}K_{33}\right)^{1/2}\frac{1}{LP_o} \qquad (2)$$

In Eq. 2, ω is the frequency of the applied field, K_{22} and K_{33} the Frank elastic constants for twist and bend, τ the space charge dielectric relaxation time related to the critical frequency ω_c for the observation of the conduction regime,

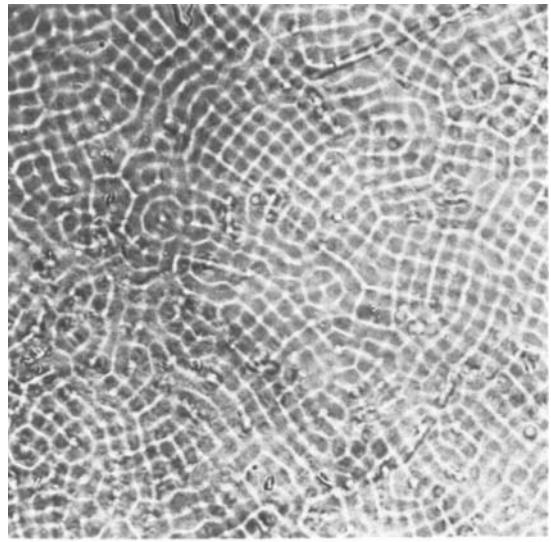

(a)

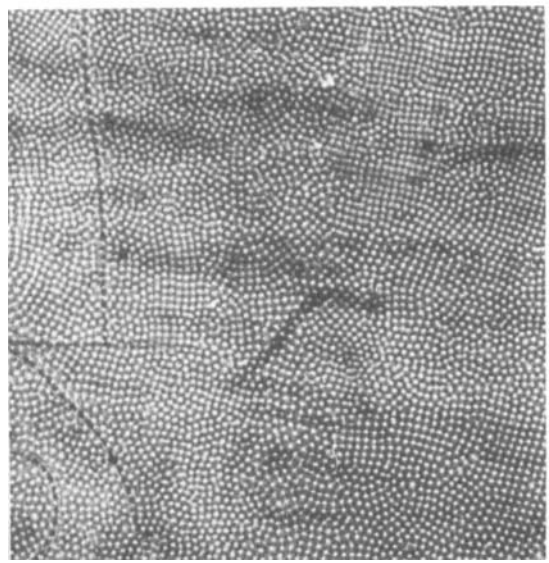

(b)

FIGURE 2 Microscopic observations at threshold on a mixture MBBA/2% CC. (a) conduction regime (b) dielectric regime (room temperature, $L = 20\ \mu m$). Magnification 175×.

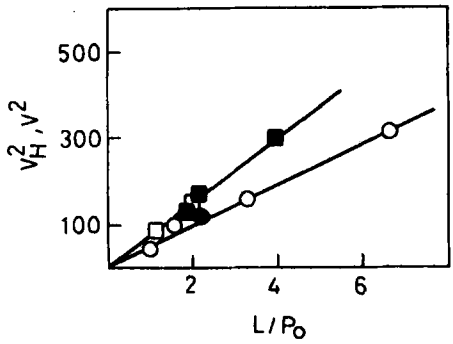

FIGURE 3 Conduction regime: square of the threshold voltage vs L/P_o (open points: MBBA/CC mixtures, full points: MBBA/CB mixtures). □ ■ fresh samples, ○ ● aged samples.

$$\tau = \frac{\varepsilon_\parallel + \varepsilon_\perp}{4\pi(\sigma_\parallel + \sigma_\perp)} = \frac{(\zeta - 1)^{1/2}}{\omega_c} \tag{3}$$

and ζ is a positive dimensionless coefficient given by

$$\zeta = 1 - \left[\frac{\sigma_\parallel - \sigma_\perp}{\sigma_\parallel + \sigma_\perp}\frac{\varepsilon_\parallel + \varepsilon_\perp}{\varepsilon_\parallel - \varepsilon_\perp}\right] \tag{4}$$

($\sigma_\parallel$ and $\sigma_\perp$ are the conductivities parallel and perpendicular to the local director axis). At threshold, the distortion is nucleated with a wavelength λ given by

$$\lambda = \left[\left(\frac{3}{2}\frac{K_{33}}{K_{22}}\right)^{1/2} P_o L\right]^{1/2} \tag{5}$$

Estimating pure MBBA-like values for $\sigma_\parallel/\sigma_\perp$, $\varepsilon_\parallel$ and $\varepsilon_\perp$[12] we obtain from Eq. 4 $\zeta = 4.25$. If we consider cut-off frequencies $f_c = \omega_c/2\pi$ of 20 and 100 Hz for fresh and aged samples respectively, we find dielectric relaxation times τ of the order of 14 and 3 msec. From the slope of the plots V_H^2 vs L/P_o (Figure 3) and from the periodicity of the distortion (MBBA/2% CC, MBBA/2% CB) we obtain for fresh and aged samples respectively: $K_{22} \cdot K_{33} = 1.99 \times 10^{-12}$ and 1.07×10^{-12} dynes^2, $K_{33}/K_{22} = 6.2$ and 8.1. The elastic constants of twist and bend can be evaluated to be of the order: $K_{22} = 5.6 \times 10^{-7}$ dynes, $K_{33} = 3.5 \times 10^{-6}$ dynes (fresh samples); $K_{22} = 3.6 \times 10^{-7}$ dynes, $K_{33} = 3.0 \times 10^{-6}$ dynes (aged samples). The twist modulus appears to be qualitatively in agreement with other data on MBBA reported in the literature;[3,5,30] the bend modulus is satisfactorily comparable with the value derived from the Carr-Helfrich instability in the

pure nematic.[12] The smaller value of K_{22} derived with aged samples can be justified on the basis of a renormalization of the modulus of isothermal compressibility due to the presence of impurities in the liquid crystal.[31]

In the dielectric regime there is a field threshold that varies with the excitation frequency as shown in Figure 1; according to Arnould-Netillard and Rondelez[5] we observe periodic and bidimensional patterns of different geometries (square or hexagonal symmetry). In Figure 4, the square of the threshold voltage for the appearance of dielectric instabilities in MBBA/CC mixtures is plotted as a function of frequency for different pitches. V_{DR}^2 appears to be more pitch-dependent than previously reported.[5] No detailed investigation of the distortion wavelength of the dielectric instability was carried out; qualitatively, λ appears to increase weakly with frequency (aged samples, f_c = 100 Hz).

The frequency dependence of the threshold voltages for doped S1014 is reported in Figure 5a. In this case (large negative ε_a), the square grid pattern of the conduction regime (threshold V_H) is not followed by space charge induced turbulence, but by the restoring of a new planar texture. The square grid pattern changes as the voltage is raised above the threshold tending to a polygonal cholesteric texture; however, under still increasing fields, this perturbed structure gradually changes to a new, incomplete planar texture with disclination threads. Assuming for the physical parameters $\varepsilon_\parallel$, $\varepsilon_\perp$, ε_a and $\sigma_\parallel/\sigma_\perp$ the values[12] of undoped S1014 and applying Hurault's approach[27] to the threshold voltages for the square grid perturbation of different mixtures (Figure 6), we derive $K_{22} \cdot K_{33} = 1.3 \pm 0.5 \times 10^{-12}$

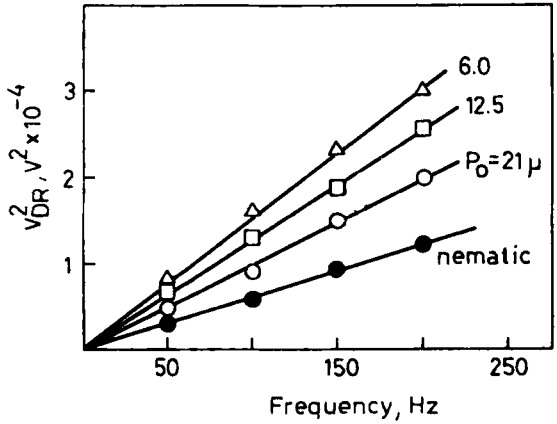

FIGURE 4 Dielectric regime: square of the threshold voltage vs frequency (MBBA/CC mixtures, sample thickness 25 μm).

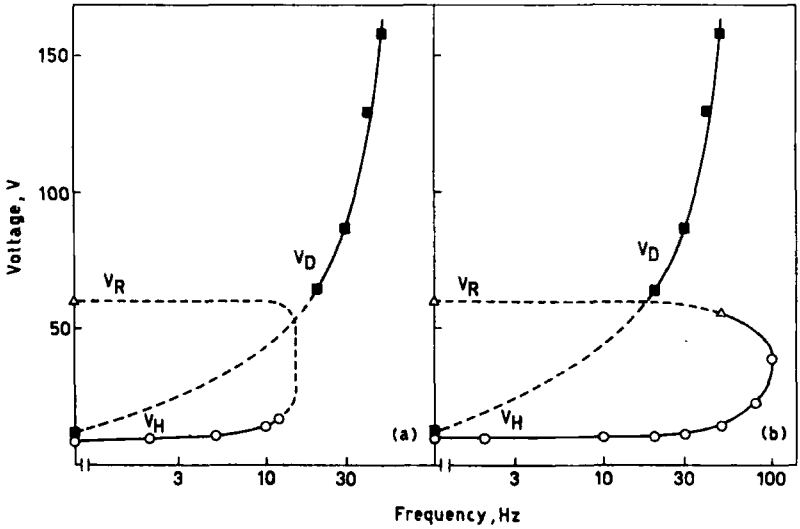

FIGURE 5 Frequency dependence of the threshold voltages for S1014/1.5% CB (40°C, sample thickness 50 μm). (a) conduction and dielectric modes in a normal sample: ○ V_H threshold of the square grid pattern, △ V_R restoring of a new planar texture, ■ V_D threshold of the dielectric regime; (b) conduction regime in a sample of increased conductivity due to ionic additives: ○ V_H threshold of the square grid pattern, △ V_R restoring of a new planar texture.

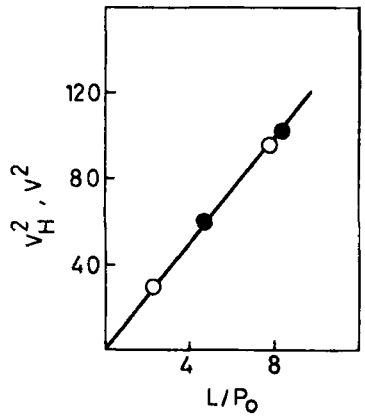

FIGURE 6 Conduction regime: square of the threshold voltage V_H vs L/P_o (open points S1014/CC mixtures, full points S1014/CB mixtures).

dynes[2]. K_{33} can be deduced from the Helfrich deformation of the pure nematic ($6.5 \pm 1 \times 10^{-6}$ dynes[12]); thus we find $K_{22} = 2.0 \pm 0.5 \times 10^{-7}$ dynes.

Considering the AC field-induced distortion in cholesteric liquid crystals of large negative dielectric anisotropy, De Zwart[32] observed several times in succession at higher voltages the formation of a new planar texture in which the original number of helices across the layer was increased by one.

We are unable to observe successively induced planar regions in our mixtures. The behavior of doped S1014 appears to be very like that reported for pure S1014.[12] Under DC excitation, we reveal a threshold for the onset of the square grid deformation V_H, a threshold for the restoring of a new planar texture V_R and, in some regions of the samples, a zero-frequency dielectric threshold V_D very close to the first threshold V_H (V_D ($\omega = 0$) must be unobservable since it lies within the instability region of the conduction mode). Increasing the conductivity of the sample with ionic additives (Figure 5b), the conduction regime moves outward in frequency and the total threshold curve becomes strongly s-shaped, due to the cross-over of the two instability modes.

(b) Small positive dielectric anisotropy.

The two-dimensional periodic pattern of the conduction regime, which can be observed both with negative and small positive ε_a is not,[6] in the case of nematic/cholesteric mixtures of weakly positive dielectric anisotropy, confined in a region of the field-frequency plane below a critical pulsation ω_c, but appears in the whole range of frequency investigated (0–10^4 Hz). As expected, the threshold voltage V_H increases with frequency and reaches a saturation value for $\omega\tau \gg 1$. The behavior of a mixture NP1052/1% CC is displayed in Figure 7. Upon increasing the voltage above V_H at a threshold V_p the helical axis is turned from the original position parallel to the field and the grid pattern deformation is replaced by the irregular polygonal texture with orientations of the helical axis varying from place to place; this configuration gradually reverts to a planar cholesteric texture with oily streaks if the field is switched off. Now the cholesteric-pseudolayers are mainly in oblique positions with respect to the electrodes and to the applied field; at higher voltages the angle between the field direction and the helical

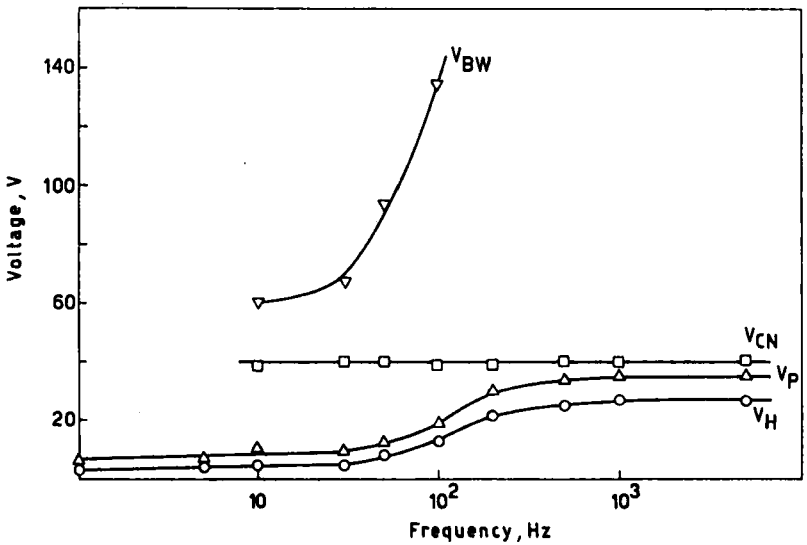

FIGURE 7 Frequency dependence of the threshold voltages for NP1052/1% CC (room temperature, sample thickness 30 μm). V_H threshold of the square grid pattern, V_P threshold of the polygonal texture, V_{CN} cholesteric to nematic transition, V_{BW} threshold for the onset of butterfly wing-like instabilities.

axis increases. At the same time, since ε_a is positive, the helix is gradually unwound by increasing the pitch until, at the critical voltage V_{CN}, the helix has vanished leading to a homeotropic nematic phase. Increasing the voltage above V_{CN}, when we reach a critical threshold V_{BW}, a distortion of the homeotropic alignment occurs in the form of localized conduction instabilities, looking like butterfly wings or coffee beans, as previously described.[12] When the field is turned off, the isotropic-like nematic texture reverts to the cholesteric polygonal texture.

According to Hurault's approach,[27] similarly to the case $\varepsilon_a < 0$, the threshold E_H for the nucleation of a static Helfrich distortion can be written in the form

$$E_H^2(\omega) = \frac{8\pi^3}{\varepsilon_\perp}\frac{\varepsilon_\parallel + \varepsilon_\perp}{\varepsilon_\parallel - \varepsilon_\perp}\frac{1 + \omega^2\tau^2}{1 - \zeta + \omega^2\tau^2}\left(\frac{3}{2}K_{22}K_{33}\right)^{1/2}\frac{1}{LP_o} \tag{6}$$

Provided that ω is sufficiently large, we can assume that E_H is practically independent of frequency and given by

$$E_H^2(\omega \to \infty) = \frac{8\pi^3}{\varepsilon_\perp}\frac{\varepsilon_\parallel + \varepsilon_\perp}{\varepsilon_\parallel - \varepsilon_\perp}\left(\frac{3}{2}K_{22}K_{33}\right)^{1/2}\frac{1}{LP_o} \tag{7}$$

The dimensionless coefficient ζ and the wavelength of the distortion are always given by Eq. 4 and 5.

The frequency dependences of V_H for mixtures NP1052/CB and NP1052/CC of different ratios L/P_o (pitches from 22.0 to 1.5 μm) are reported respectively in Figures 8 and 9; the plots V_H^2 ($\omega \rightarrow \infty$) vs L/P_o are inserted. In the case of CB mixtures, V_H^2 increases linearly with L/P_o, as predicted by Eq. 7; however, if we consider the mixture with 10%CB ($L/P_o = 20$, $P_o = 1.5$ μm) the plateau expected from a linear extrapolation of V_H^2 ($\simeq$123 Vrms) is not experimentally observed and V_H increases with frequency, resembling the behavior of a mixture of negative ε_a. We could suppose that at high concentration of CB in the nematic NP1052, ε_a changes sign; this observation might be reasonable as long as a cholesteric dopant with $\varepsilon_a < 0$ is dissolved in a nematic matrix with ε_a close to zero.

The behavior of NP1052/CC mixtures is quite different; V_H ($\omega \rightarrow \infty$) increases with L/P_o for large values of the cholesteric pitch (1-2% CC), but decreases abruptly when the pitch becomes smaller (5-10% CC). In Figure 10, the squares of the threshold voltages V_H ($\omega \rightarrow \infty$) are normalized to the sample thickness and plotted as a function of the inverse of the natural pitch P_o. For CB mixtures, V_H^2/L is found proportional to P_o^{-1}; the slope of this plot is related to the product $K_{22} \cdot K_{33}$ of the elastic constants for twist

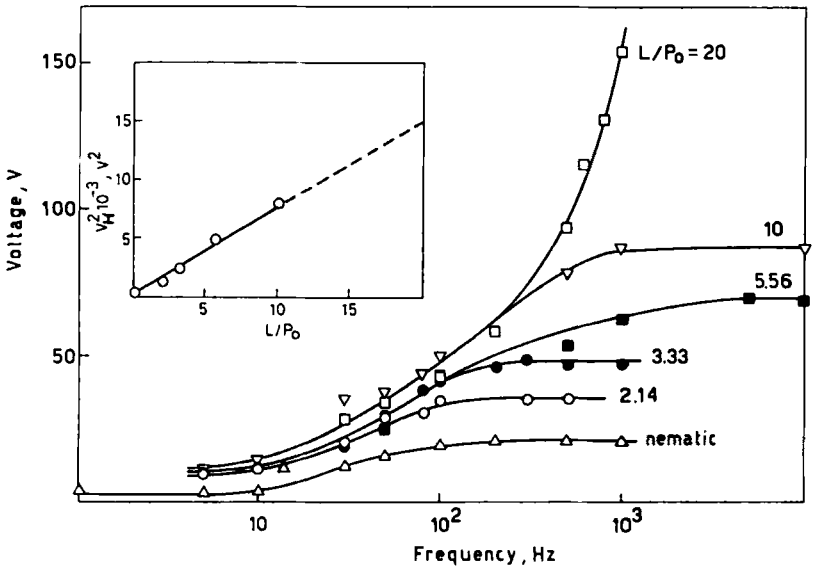

FIGURE 8 Frequency dependence of V_H for mixtures NP1052/CB with different ratios L/P_o (natural pitches of 14, 9, 3 and 1.5 μm). The plot V_H^2 ($\omega \rightarrow \infty$) vs L/P_o is inserted.

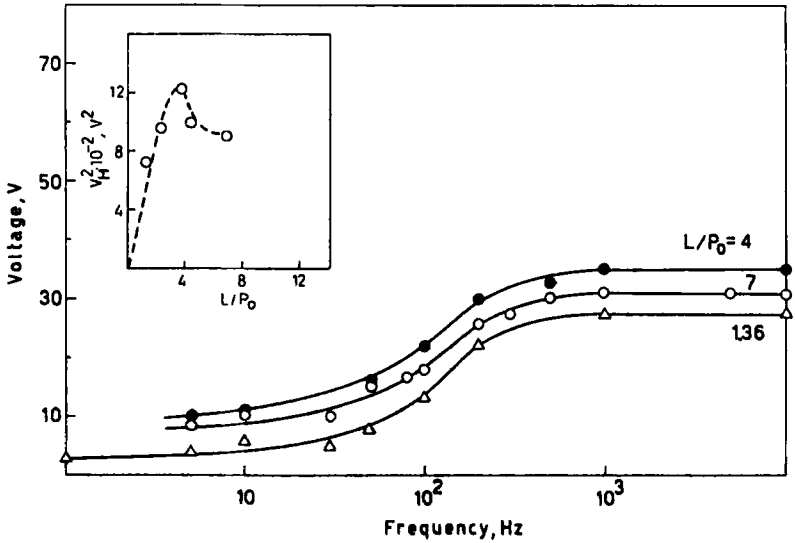

FIGURE 9 Frequency dependence of V_H for mixtures NP1052/CC with different ratios L/P_o (natural pitches of 22, 12.5 and 4.3 μm). The plot V_H^2 ($\omega \rightarrow \infty$) vs L/P_o is inserted.

and bend deformations. Assuming pure NP1052-like values for ε_a, $\varepsilon_\perp$ and $\varepsilon_\parallel$[12] at low concentrations of the cholesteric dopant, we obtain $K_{22} \cdot K_{33} = 1.89 \times 10^{-12}$ dynes.[2] On the contrary, in the case of CC mixtures, the product $K_{22} \cdot K_{33}$ appears to be strongly pitch dependent. From the wavelength of the deformation at threshold, we can derive the ratio of the two elastic constants. Combining these data with the results for the product $K_{22} \cdot K_{33}$ we determine K_{22} and K_{33} for different mixtures. The calculated values are reported in Table II. K_{33} is in relatively good agreement with the value[12] derived from the Helfrich threshold of undoped NP1052 ($3.9 \pm 1 \times 10^{-6}$ dynes); the twist modulus K_{22} varies with the cholesteric dopant and for CC mixtures decreases strongly, decreasing the cholesteric pitch of the sample.

When the applied field is raised to the threshold V_p (see Figure 7), the cholesteric arrangement of CC and CB mixtures corresponds to the tilted polygonal texture; in mixtures of small natural pitch ($P_o < 5$ μm), V_p indicates a helical axis rotation to a focal conic state. At threshold, the neighboring domains are not well defined; under increasing fields, dislocation lines are visible which separate regions of different orientation of

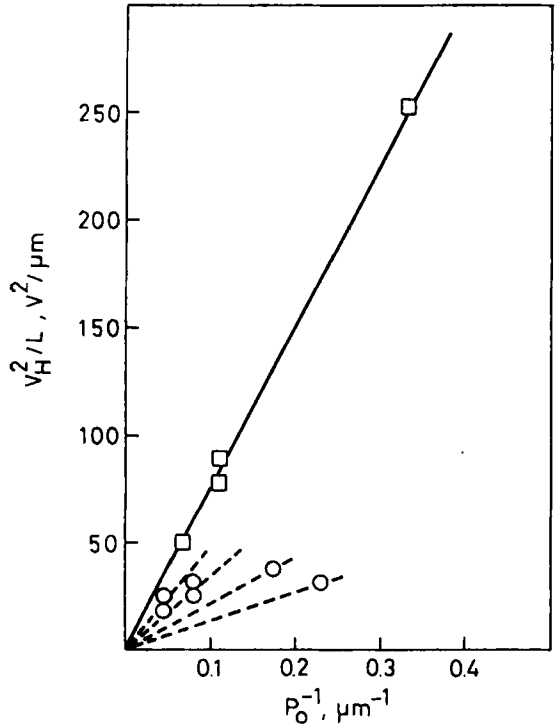

FIGURE 10 Square of the threshold voltage V_H normalized to the sample thickness vs reciprocal pitch (□ NP1052/CB mixtures, ○ NP1052/CC mixtures).

Table II

Determination of the twist and bend elastic modules from the threshold voltage and the wavelength of the square grid deformation (doped NP1052)

Cholesteric dopant	P_0, μm	$K_{22} \cdot K_{33} \times 10^{12}$, dynes^2	λ^2/LP_0	K_{33}/K_{22}	$K_{22} \times 10^7$, dynes	$K_{33} \times 10^6$, dynes
CB 1-6%	14-3	1.89			4.77	3.96
CB 2%	9		3.53	8.3		
CC 1%	22	0.77	6.72	30.2	1.59	4.81
CC 2%	12.5	0.40	8.15	44.3	0.95	4.21
CC 5%	5.7	0.15	9.90	65.3	0.48	3.13
CC 10%	4.3	0.064				

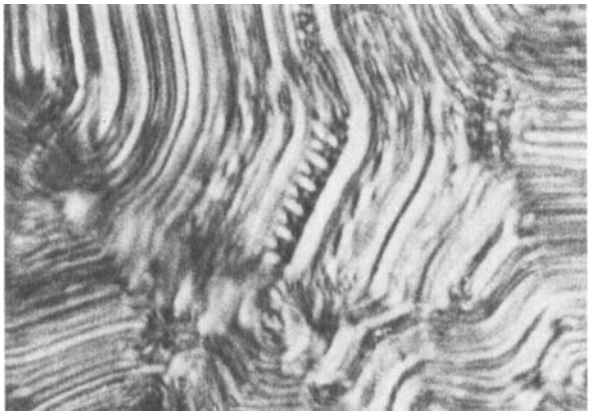

FIGURE 11 Microscopic observation on a "defect" in the polygonal texture of NP1052/1% CC. (Sample thickness 50 μm; 550×).

the helical axis. In the bulk of the sample we can observe a number of "defects" (as depicted in Figure 11) which vanish gradually at higher fields. In mixtures containing small amounts of the cholesteric dopants, our sample thickness is some small multiple of the pitch. In this situation we must take into account the role played by the boundary conditions; because of the finite penetration length, they will cause a strong bending of the cholesteric layers. For a small tilt angle, the layers are simply curved; when this angle increases with increasing voltage, the layers intersect each other and typical features, as in Figure 11, appear.

Under still increasing fields, a distortion of the helical structure occurs. The apparent pitch, which is essentially unperturbed at low voltages, dilates first very slowly and then diverges logarithmically for $V = V_{CN}$. Beyond V_{CN} the cholesteric liquid crystal transforms into a nematic.

Microscopic observations of the unwinding of the cholesteric helix are reported in Figure 12 for a mixture NP1052/1% CC. The reduced pitch, P/P_i vs the reduced voltage V/V_{CN} is shown in Figure 13. P_i represents the average value of the apparent pitches before the beginning of helix expansion; in our experimental situation, this is generally smaller than the natural values P_o, due to the mainly oblique position of the cholesteric pseudolayers with respect to the glass electrodes. P values at different voltages are averaged over many experimental determinations.

De Gennes[33] and Meyer[34] demonstrate that complete unwinding of the cholesteric is induced above a threshold

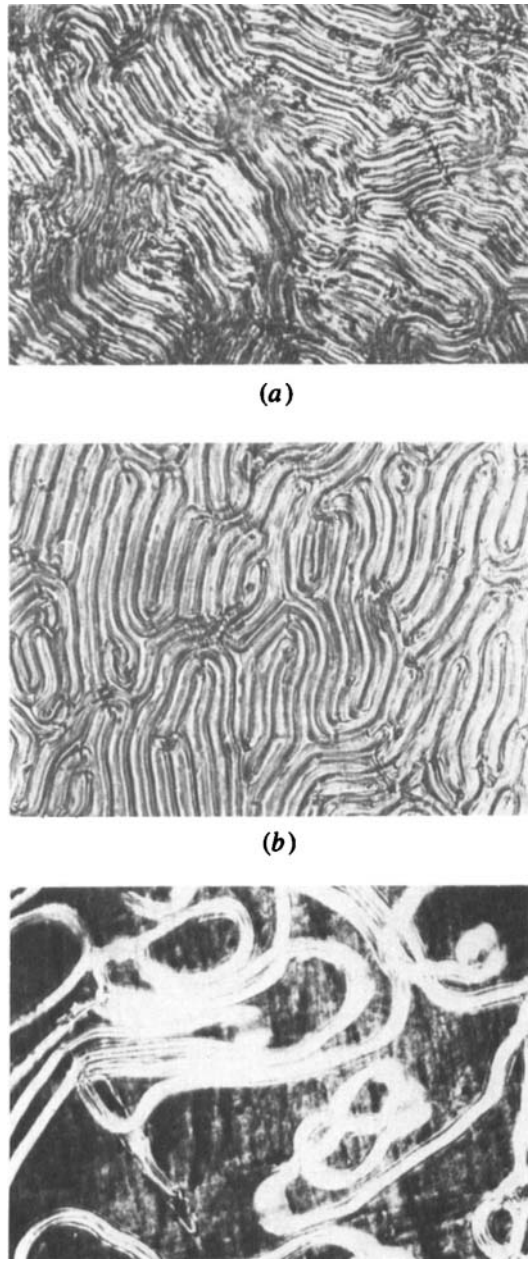

(a)

(b)

(c)

FIGURE 12 Microscopic observations on the unwinding of the cholesteric helix (NP1052/2% CC; $L = 50\ \mu m$). (a) $V \simeq V_p$; (b) $V \simeq V_{CN}$; (c) $V > V_{CN}$ — 175×.

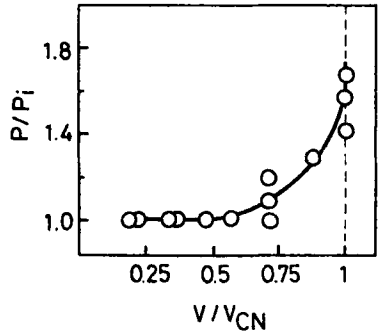

FIGURE 13 Reduced pitch P/P_i as a function of the reduced voltage V/V_{CN} (NP1052/2% CB; $L = 50$ μm).

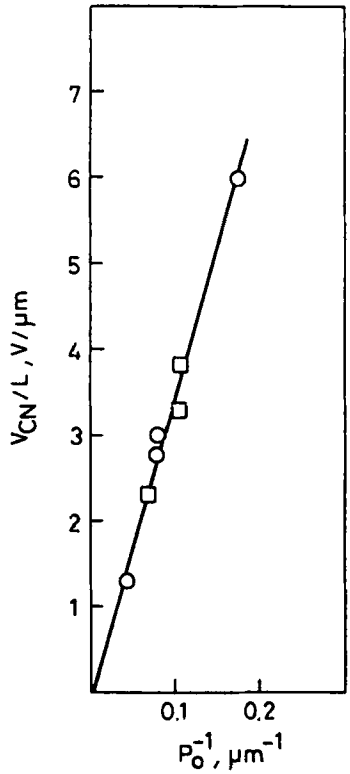

FIGURE 14 Cholesteric to nematic transition: threshold voltage normalized to the sample thickness as a function of the reciprocal pitch (□ NP1052/CB mixtures, ○ NP1052/CC mixtures).

$$V_{CN} = 2\pi^2 \left(\frac{\pi K_{22}}{\varepsilon_a}\right)^{1/2} \frac{L}{P_o} \tag{8}$$

The variation of V_{CN}/L vs P_o^{-1} for NP1052/CC and NP1052/CB mixtures is shown in Figure 14. We are unable to detect this field-induced phase transition in samples with too small a pitch; qualitative results refer to P_o values from 22 to 5.7 μm (CC 1, 2, 5%, CB 1, 2%). However, it is quite surprising to derive a twist elastic modulus K_{22} of $11 \pm 2 \times 10^{-7}$ dynes, independent of the nature and the amount of the cholesteric dopant. It does not compare with the preceding determinations using V_H.

We can try to discuss this anomalous result taking into account some quantities involved in Eqs. 7 and 8 respectively. Generally it is assumed that small amounts of a cholesteric dopant do not affect the dielectric constants and ε_a of the nematic matrix. However, this approximation would be not valid in the case of NP1052 whose dielectric anisotropy is close to zero. We have just mentioned that a mixture containing 10% CB resembles a cholesteric liquid crystal with negative ε_a; CC is expected to maintain or more probably to increase the positive anisotropy of NP1052. Eqs. 7 and 8 show that the thresholds V_H and V_{CN} are respectively proportional to $(\varepsilon_\parallel + \varepsilon_\perp)/\varepsilon_\perp\varepsilon_a$ and $1/\varepsilon_a$. These two terms might be differently affected by the presence of increasing amounts of CC in the mixture.

Another quantity to consider is, in our opinion, the threshold voltage of the cholesteric to nematic transition. We can take into account non-uniform distortions during the cholesteric spiral untwisting; Meyer[10] observed that in a real sample strongly interacting with the walls, the dynamics of the distortion of the helical structure must be non-uniform. As evidence for this non-uniformity, he mentioned a threshold field greater than the critical one in samples where a few alignment inversion walls were present. Additional reports of non-uniform distortions during electric field induced unwinding of the cholesteric are in the literature.[35-37]

Recently, Asai, *et al.*,[38] indicate that the de Gennes model for field-induced cholesteric-nematic phase change[33] can be applied to determine the pitch change and the critical field, but not to express the actual deformation. These authors prove that a new parameter including the tilt angle in the direction of the helical axis is more suitable for evaluating the deformation, since the molecules are tilted along the helical axis under the influence of the surface treatment.

Theoretical discussions leading to Eq. 8 consider a situation of pure twist with the helical axis normal to the field. This is indeed the usual situation for homeotropically aligned cholesteric slabs. However, in the case of oblique positions of the cholesteric pseudolayers with respect to the applied field (tilt angle $< 90°$), the one-dimensional situation of pure twist can no

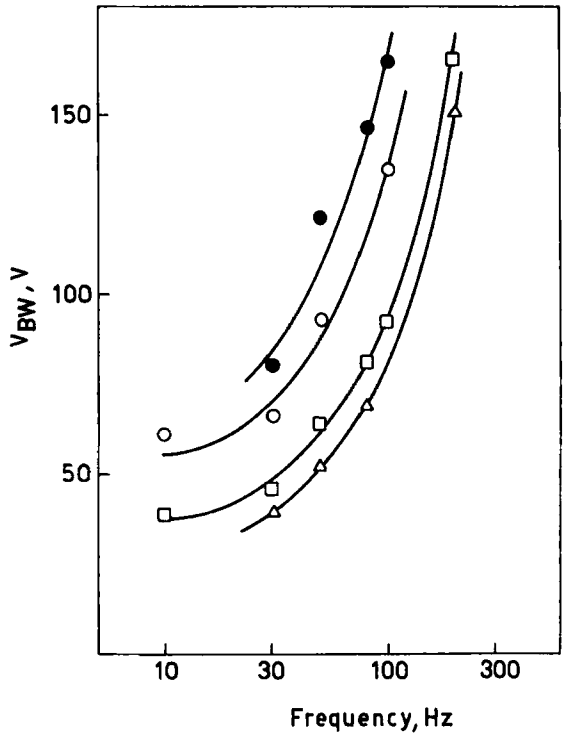

FIGURE 15 Frequency dependence of the threshold voltage for the onset of conduction instabilities (V_{BW}) in doped NP1052 transformed to the nematic state with homeotropic configuration by the applied field (○ 1% CC, ● 2% CC, △ 2% CB, □ pure nematic; sample thickness 30 μm).

longer be assumed; in addition the experimental threshold is probably overvalued, since only one component of the applied field is effective in favorably orientating the molecules along the field. The dielectric constant measured along the helical axis is $\varepsilon_\perp$; when measured normal to the helical axis it is the average $\frac{1}{2}(\varepsilon_\parallel + \varepsilon_\perp)$. In the case of doped NP1052, this average should be very little larger than $\varepsilon_\perp$; in consequence, the tendency of the helical axis to orient normal to the applied field should be weak. From the comparison between the apparent pitches P_i and the unperturbed pitches P_o, we can evaluate tilt angles of 50 and 25–30° for CB and CC mixtures respectively. Calculating with Eq. 8 the expected threshold using the twist elastic constants derived from the Helfrich distortion and comparing these data with the experimental values of V_{CN}, we find tilt angles of about 60 and 20° for CB and CC mixtures. The agreement between the data is not too good,

probably due to the poor experimental accuracy in the evaluation of P_i which is not quite constant in different domains. However, we feel that the principal cause of the anomalous results for K_{22} derived from the thesholds V_{CN} arises from different tilt angles of the helical structure in CB and CC mixtures, which can be related to the relative values of the dielectric constants, to surface interactions, to the different ability of CB and CC to twist the nematic phase, and to the different twist modules.

The behavior of doped NP1052 transformed to a nematic state with a homeotropic configuration is shown in Figure 15 and compared with pure NP1052. The experimental points identify a shift of the threshold curve toward higher voltages with increasing amounts of CC in the nematic; on the other hand, in a 2% CB mixture, instabilities are observed at a threshold a little smaller than in the pure nematic. The cholesteric dopants in this configuration can in our opinion only affect the dielectric constants and the

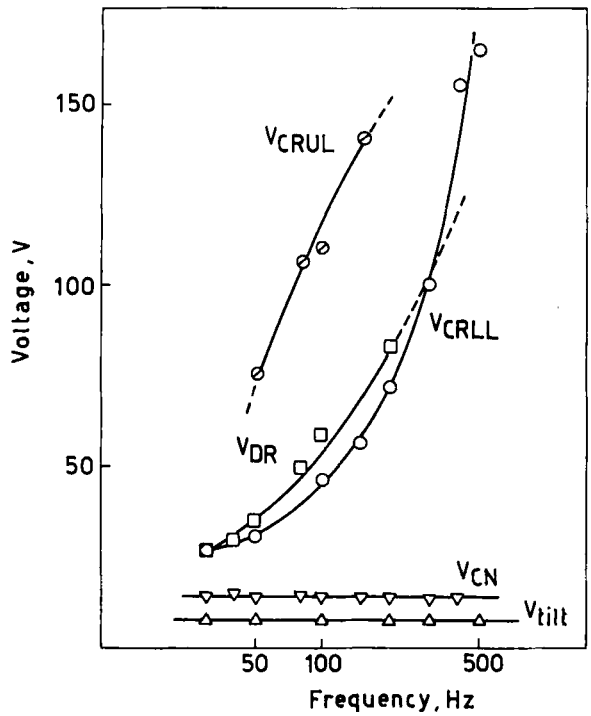

FIGURE 16 Frequency dependence of the threshold voltages for PEBAB/4% CB (T = 120°C, sample thickness 50 μm). V_{tilt} tilting over to a finger print texture, V_{CN} cholesteric to nematic transition, V_{CRLL} and V_{CRUL} lower and upper limits of the splay conduction mode, V_{DR} splay dielectric regime.

conductivities of the nematic phase. We suggest that the principal effect is a variation of the dielectric anisotropy which is reduced by CB and increased by CC. We cannot verify such an effect since theoretical predictions about positive nematics in the homeotropic alignment[39] do not lead to an analytical form for the threshold line.

(c) Large positive dielectric anisotropy.

Figure 16 refers to the response of doped PEBAB (4% CB) in the planar configuration to an externally applied AC field. Due to its positive ε_a, the system tends to orient with the cholesteric planes parallel to the field; as a consequence, the helical axis is turned $\pi/2$ from the original position parallel to the field at a threshold of few volts. Now the field is applied at right angles to the helical axis; as the voltage approaches the critical value V_{CN} the pitch increases logarithmically; for $V > V_{CN}$ the helix is destroyed completely and the structure becomes nematic. In mixtures with high positive ε_a, V_{CN} can be as low as a few volts. Optically, the slabs look clear under ordinary light and isotropic-like between crossed polarizers (homeo-

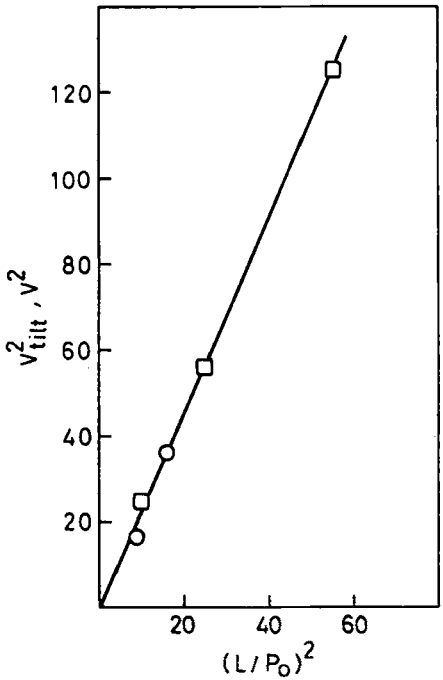

FIGURE 17 $V^2_{tilt(\square\,CB,\,\circ\,CC)}$ as a function of $(L/P_o)^2$. PEBAB mixtures.

tropic configuration). Extinction is maintained when the sample is rotated around the optic axis. Increasing the voltage above V_{CN}, a distortion of the homeotropic alignment occurs at a threshold V_{CRLL}. Butterfly wing-like or coffee bean-shaped conduction instabilities appear from zero to a cut-off frequency. At higher voltage (V_{DR}), a splay dielectric regime in the form of a few μm-period square grid is observed, whose wave vector is strongly frequency dependent. The domain of existence of the conduction mode appears to be a closed loop in a voltage/frequency plane, since it has a lower threshold V_{CRLL} at which instabilities appear and an upper limiting voltage V_{CRUL} above which only the dielectric mode is distinguishable; the low frequency dielectric threshold intersects the instability region of the conduction regime. The observed behavior agrees with theoretical predictions[39] and with our previous results on undoped PEBAB and S1016.[12] When the field is turned off the liquid crystal returns to the twisted state.

Now we consider in detail the different deformations occurring at different values of the AC voltage and the threshold dependences on the sample thickness and the cholesteric pitch.

The tilting over to a fingerprint texture is the lower threshold given by[11]

$$V_{tilt} = 4\pi\left(\frac{K_{22}\pi}{\varepsilon_a}\right)^{1/2} L/P_o \tag{9}$$

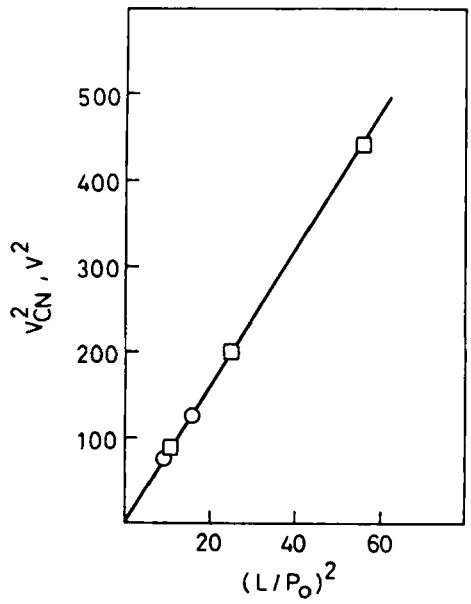

FIGURE 18 $V^2_{CN(\square\,CB,\,\circ\,CC)}$ as a function of $(L/P_o)^2$. PEBAB mixtures.

The correlation of V_{tilt} with the ratio L/P_o (Figure 17) leads to an evaluation of the twist elastic constant of PEBAB in the order of 8×10^{-7} dynes. The unwinding of the helical structure is induced at the threshold voltage V_{CN}; from the slope of the plot V_{CN}^2 vs $(L/P_o)^2$ (Figure 18), we derive $K_{22} = 11 \times 10^{-7}$ dynes.

These results refer to cholesteric layers thicker than the pitch of the helix. If $P_o > L$ only a deformation of the Fréedericksz type is observed above a theshold voltage V_{FT} given by[1]

$$V_{FT} = \left(\frac{K_{11}4\pi^3}{\varepsilon_a} + \frac{K_{33}16\pi^3}{\varepsilon_a}\frac{L^2}{P_0^2}\right)^{1/2}. \tag{10}$$

where K_{11} is the elastic modulus of splay. Our experimental accuracy on this determination is very poor; from the few samples investigated (1% CC mixture, sample thickness 30–50 μm) we obtain a rough evaluation of the bend elastic constant of PEBAB in the order of 5×10^{-6} dynes, assuming for K_{11} a value of 1.3×10^{-6} dynes, derived from the Fréedericksz transition of the undoped nematic.[12]

Figure 19 refers to the behavior of doped PEBAB transformed to the nematic state by the applied field. The threshold curve for the appearance of the splay conduction mode (left side of the figure) appears to be independent of the type and the amount of the cholesteric dopant; it reproduces the trend reported for pure PEBAB.[12] As revealed by the undoped nematic, the cut-off frequency shifts toward higher values when the thickness is decreased. In the dielectric regime, the analogy with the behavior of pure PEBAB is also striking; as previously discussed,[12] in this case we are dealing with a field threshold (right side of Figure 19). Probably due to the small periodicity of the pattern, it is difficult to detect the onset of the square grid of splay in the high frequency region.

We can conclude that PEBAB/CC and PEBAB/CB mixtures behave in a similar way under an AC applied field; due to the high values of ε_a, $\varepsilon_\parallel$ and $\varepsilon_\perp$ the cholesteric dopants do not affect these physical parameters of the nematic matrix. Probably they act on the conductivity and on the induced deterioration of the liquid crystal which appears more stable chemically in mixtures than in the undoped state.

The behavior of doped S1016 appears to be quite similar to that reported for PEBAB mixtures. An electric field strong enough to overcome any influence of the walls aligns the helical axis perpendicular to itself; a twist modulus in the order of 3.5×10^{-6} dynes is obtained. As the voltage rises, in the region of alignment parallel to the field, the pitch increases logarithmically and we obtain a nematic structure; from the theshold V_{CN} we

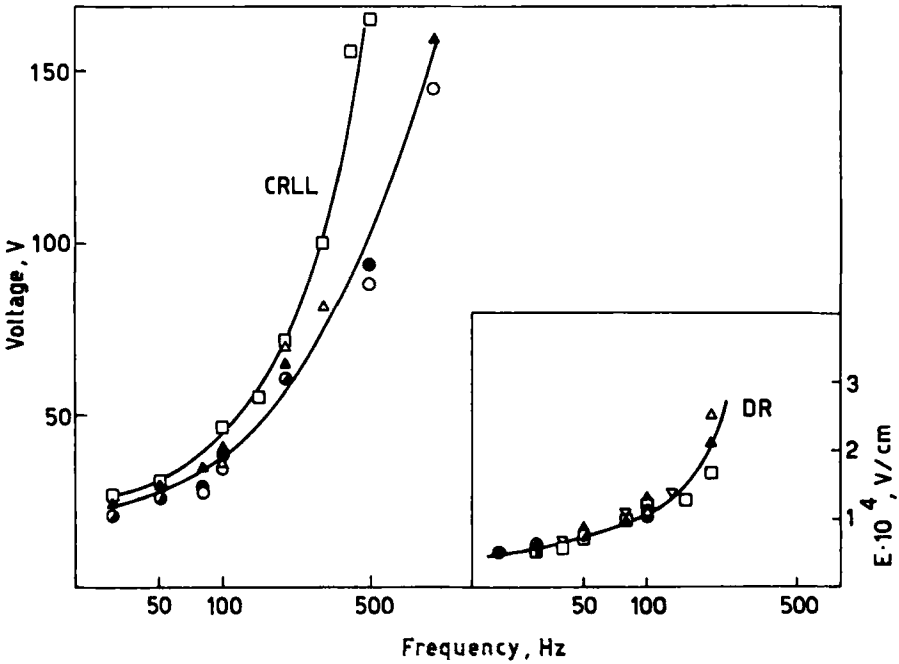

FIGURE 19 Doped PEBAB transformed to the homeotropic nematic state. Left side: threshold voltage of the lower limit of the conduction regime; right side: threshold field of the dielectric regime. (L = 30 μm: ○ 4% CB, △ 10% CB, ● 1% CC, ▲ 10% CC. L = 50 μm: □ 4% CB, ▽ pure nematic).

derive for K_{22} a value of about 5.5×10^{-6} dynes. In the homeotropic configuration, instabilities occur as reported for undoped S1016.[12]

The agreement between K_{22} values derived from V_{tilt} and V_{CN} in both doped PEBAB and S1016 is quite good, considering the impossibility of determining accurately the threshold voltage for the $\pi/2$ rotation of the helical axis.

CONCLUSIONS

The results we have reported concern the effect of dielectric anisotropy on the response of nematic/cholesteric mixtures, in a planar alignment, to an electric field applied along the helical axis. The behavior of samples of negative or large positive dielectric anisotropy appears to be in relatively

good agreement with theoretical predictions and literature experimental reports. K_{22} decreases when impurities are present.

An uncommon effect is found in the case of a small positive ε_a; the threshold voltage for the appearance of the square grid pattern is influenced by the nature and the amount of the cholesteric dopant. Applying Hurault's approach we evaluate a single twist modulus for CB mixtures, and different values of K_{22} for each CC mixture. These results do not compare with the derivation of K_{22} from the threshold voltage of the cholesteric-nematic transition. The anomalous behavior is discussed in terms of a possible variation of the dielectric constants with the cholesteric dopant; limitations upon a good determination of V_{CN} in our experimental situation are also considered.

Experiments were performed in the case $L > P_o$, $K_{33} > K_{22}$. It is well known that the cholesteric structure is remarkably influenced by the ratio L/P_o. In agreement with literature[3] reports for $\varepsilon_a \gg 0$ and $L < P_o$, a transition of the Fréedericksz type is observed, rather than the tilting to a finger print texture and helical unwinding. For $L < P_o$ and negative or small positive ε_a, in accordance with the results of Hervet *et al.*,[40] a periodic one-dimensional distortion appears, in contrast to the case $L > P_o$, where a square grid pattern is nucleated under the same conditions.

Acknowledgment

This investigation was supported by Ministero Pubblica Istruzione.

References

1. H. Kelker and R. Hatz, Handbook of Liquid Crystals, Verlag Chemie, Weiheim (1980), Chap. 4, pp. 207–217.
2. K. Yoshino, K. Yamashiro and Y. Inuishi, *Jpn. J. Appl. Phys.*, **13**, 1471 (1974).
3. P. G. de Gennes, The Physics of Liquid Crystals, Oxford Univ. Press, London (1974).
4. W. Haas, J. Adams and J. B. Flannery, *Phys. Rev. Lett.*, **24**, 577 (1970).
5. H. Arnould-Netillard and F. Rondelez, *Mol. Cryst. Liq. Cryst.*, **26**, 11 (1974).
6. F. Rondelez, H. Arnould and C. J. Gerritsma, *Phys. Rev. Lett.*, **28**, 735 (1972).
7. J. J. Wysocki, J. Adams and W. Haas, *Mol. Cryst.*, **8**, 471 (1969).
8. J. J. Wysocki, J. Adams and W. Haas, *Phys. Rev. Lett.*, **20**, 1024 (1968).
9. H. Baessler and M. M. Labes, *Phys. Rev. Lett.*, **21**, 1791 (1968).
10. R. B. Meyer, *Appl. Phys. Lett.*, **14**, 208 (1969).
11. R. Bartolino, A. Ruffolo, F. Simoni and N. Scaramuzza, *Il Nuovo Cimento*, **1**, 607 (1982).
12. M. L. Sartirana, B. Valenti and R. Bartolino, *J. Phys. (Paris)*, submitted for publication.
13. F. Grandjean, *C. R. Acad. Sci. (Paris)*, **172**, 71 (1921).
14. R. Cano, *Bull. Soc. fr. Minéral. Cristallogr.*, **911**, 20 (1968).
15. Orsay Liquid Crystal Group, *Phys. Lett.*, **28A**, 687 (1969).
16. G. Heppke and F. Oestreicher, *Z. Naturforsch.*, **32a**, 899 (1977).
17. G. P. Berthault, Thèse de Doctorat, Paris (1977).

18. H. Baessler and M. M. Labes, *J. Chem. Phys.*, **52**, 631 (1970).
19. H. W. Gibson, "*Liquid Crystals. The Fourth State of Matter*" (Ed. F. D. Saeva), Marcel Dekker Inc., New York (1979).
20. J. E. Adams and W. Haas, *Mol. Cryst. Liq. Cryst.*, **15**, 27 (1971).
21. F. D. Saeva and J. J. Wysocki, *J. Am. Chem. Soc.*, **93**, 5928 (1971).
22. J. E. Adams and L. B. Leder, *Chem. Phys. Lett.*, **6**, 90 (1970).
23. J. E. Adams, W. E. Haas and J. J. Wysocki, "*Liquid Crystals and Ordered Fluids*" (Eds. J. F. Johnson and R. S. Porter), Plenum, New York (1970).
24. Y. Bouligand, *J. Phys. (Paris)*, **33**, 715 (1972).
25. W. Helfrich, *Appl. Phys. Lett.*, **17**, 531 (1970).
26. W. Helfrich, *J. Chem. Phys.*, **52**, 839 (1971).
27. J. P. Hurault, *J. Chem. Phys.*, **59**, 2068 (1973).
28. E. Dubois-Violette, P. G. de Gennes and O. Parodi, *J. Phys. (Paris)*, **32**, 305 (1971).
29. I. W. Smith, Y. Galerne, S. T. Lagerwall, E. Dubois-Violette and G. Durand, *J. Phys. (Paris)*, **36**, 237 (1975).
30. K. Skarp and T. Carlsson, *Mol. Cryst. Liq. Cryst. Lett.*, **49**, 75 (1978).
31. P. S. Pershan and J. Prost, *J. Appl. Phys.*, **46**, 2343 (1975).
32. M. De Zwart, *J. Phys. (Paris)*, **39**, 423 (1978).
33. P. G. de Gennes, *Solid State Commun.*, **6**, 163 (1968).
34. R. B. Meyer, *Appl. Phys. Lett.*, **12**, 281 (1968).
35. C. Z. van Doorn, *Phys. Lett.*, **42A**, 537 (1973).
36. C. J. Gerritsma, W. H. de Jeu and P. van Zanten, *Phys. Lett.*, **36A**, 389 (1971).
37. L. J. Yu and M. M. Labes, *Mol. Cryst. Liq. Cryst.*, **28**, 423 (1974).
38. H. Asai, M. Terasaki, T. Hasegawa and S. Kurita, *Mol. Cryst. Liq. Cryst.*, **84**, 285 (1982).
39. E. Dubois-Violette, G. Durand, E. Guyon, P. Manneville and P. Pieranski, Liquid Crystals (Ed. L. Liebert), Supplement 14, Solid State Physics, Academic Press Inc., New York (1978).
40. H. Hervet, J. P. Hurault and F. Rondelez, *Phys. Rev.*, **A8**, 3055 (1973).